On the Saturation & Thermalization of Carbon Dioxide II

by
Joseph Reynen
jwreynen@gmail.com
Published March 05, 2022

PRINCIPIA SCIENTIFIC International

On the Saturation and Thermalization of Carbon Dioxide II

Joseph Reynen
jwreynen@gmail.com

March 05, 2022

Introduction

This paper II is an update of an earlier paper of December 02, 2021. [5]
Infra-red-active gases in the atmosphere are: water-vapor (H_2O), carbon dioxide (CO_2), methane (CH_4), ozone (O_3) , laughing gas (N_2O).....
They hinder long-wave (LW) radiation to outer space from the surface of the planet to evacuate the heat which the sun is sending to the planet as short wave (SW) radiation.
The most important infra-red active gases are H_2O vapor and CO_2 gas.
In earlier papers the author has studied the hindering of the LW evacuation of heat from the terrestrial surface to outer space by a mechanism of a stack of fine gauze, simulating the infra-red-active gases.

Stack model to study the evacuation of heat from the planet.

A finite element method (FEM) has been used.
Not in the classical way of solving differential equations, but rather using FEM strategies to model the phenomenon and to deal with a great number of simultaneous algebraic relations using matrix notations.
In [1] is given a more detailed description of the FEM based stack model.

Figure 1 Stack of fine gauze

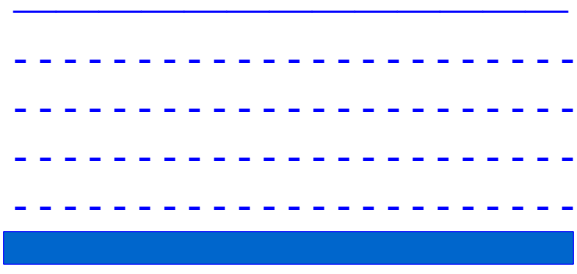

We consider in figure 1 a stack of N-2 grids, with dimensionless absorption coefficients f(i)<<1, being the ratio of the cross-section of the wires divided by the total surface.
The absorption coefficients are assembled in a vector denoted by a bold character **f** of order N, including f(1)=1 for the surface and f(N)=1 for outer-space. We define ftot =sum(**f**) - 2 , being the sum for the atmospheric grids.
Consider two layers of black grids with coefficients f(i) and f(j) , and absolute temperatures (Kelvin) T(i) and T(j) , respectively.
According to the classical Stefan-Boltzmann relation with σ = 5.67e -8, the heat flux φ by LW radiation between the two grids can be written as :

$\varphi(i \rightarrow j) = f(i)*f(j)*\sigma*(T(i)\text{^}4 - T(j)\text{^}4)$ and $\varphi(j \rightarrow i) = 0$ for T(i)>T(j) **(1)**

With $\vartheta = \sigma * T\text{^}4$ and fe = f(i)*f(j) relation (1) can be written as:

$\varphi(i \rightarrow j) = fe*(\vartheta(i)-\vartheta(j))$ and $\varphi(j \rightarrow i) = 0$ for $\vartheta(i)>\vartheta(j)$ **(1a)**

This is the one-stream energy formulation without the nonphysical back - radiation of the two-stream Schwarzschild formulation of 1916.

A radiation finite element with nodal parameters is depicted in figure 2.

Figure 2 **Radiation finite element**

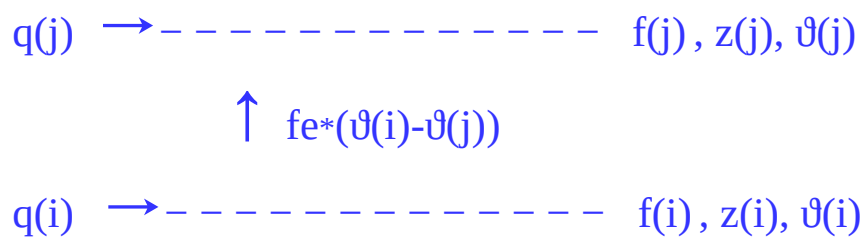

Nodal parameters : f absorption coefficient
z coordinate [km]
ϑ variable representing σ*T^4 [W/m²]
q external heat load into the grids [W/m²]
Constitutive relation : fe element radiation coefficient

By means of a Galerkin-type of variation process, the element heat balance can be written as:

$$\begin{vmatrix} q(i) \\ q(j) \end{vmatrix} = \begin{vmatrix} fe & -fe \\ -fe & fe \end{vmatrix} \begin{vmatrix} \vartheta(i) \\ \vartheta(j) \end{vmatrix} \qquad \textbf{(2)}$$

Equations **(2)** describe for given $\vartheta(i)$ and $\vartheta(j)$ the flow of heat by LW radiation between the grids i and j and the necessary external heat sources q(i) and q(j) , for a balance.
For an element with grids in adjacent levels i and j , the element transfer coefficient is indeed fe = f(i)*f(j).
However, elements of the type of figure 2 can be overlapped with each other. When between grid i and grid j of one element other grids of other elements are present, the transfer of heat by radiation between grid i and grid j will be hindered and fe becomes :

$$fe = f(i)*viewfactor(i , j)*f(j) \qquad \textbf{(2a)}$$

In **(2a)** the viewfactor(i, j) takes into account the fact that other grids k are present between grid i and grid j of an element (i, j).
The viewfactor(i, j) of the element (i, j) can be written as :

$$viewfactor(i , j) = 1 - \sum f(k) \quad \text{with} \quad z(i)<z(k)<z(j) \qquad \textbf{(2b)}$$

The element matrices for the different pairs of grids are assembled in a system matrix, denominated by a bold character **K.**
For a stack with N levels there are N(N-1)/2 pairs with a balance like **(2)** and the system matrix is of order NxN.
Nodal parameters $\vartheta(i)$ and nodal heat loads q(i) are assembled in vectors of order N , denominated with bold characters $\boldsymbol{\vartheta}$ and **q**, respectively.
The characteristic equations of the atmospheric LW radiation become :

$$\mathbf{q} = \mathbf{K}*\boldsymbol{\vartheta} \qquad \textbf{(3)}$$

The vector relation (3) represents N algebraic relations: for given values of the components of the vector $\boldsymbol{\vartheta}$ and of the matrix **K** one obtains the vector **q** of external thermal loads into the stack with sum(**q**)= 0 , for a balance.

Data for the components of the vector ϑ and the matrix K

The data for these components are shown in figure 3 :
temperature distribution and concentration of water vapor and of carbon dioxide gas over a height of 30 km..

NB *In computer language subscripts are not used. From now on, in this paper, we write not anymore* H_2O *and* CO_2 *but* H2O *and* CO2.

Figure 3

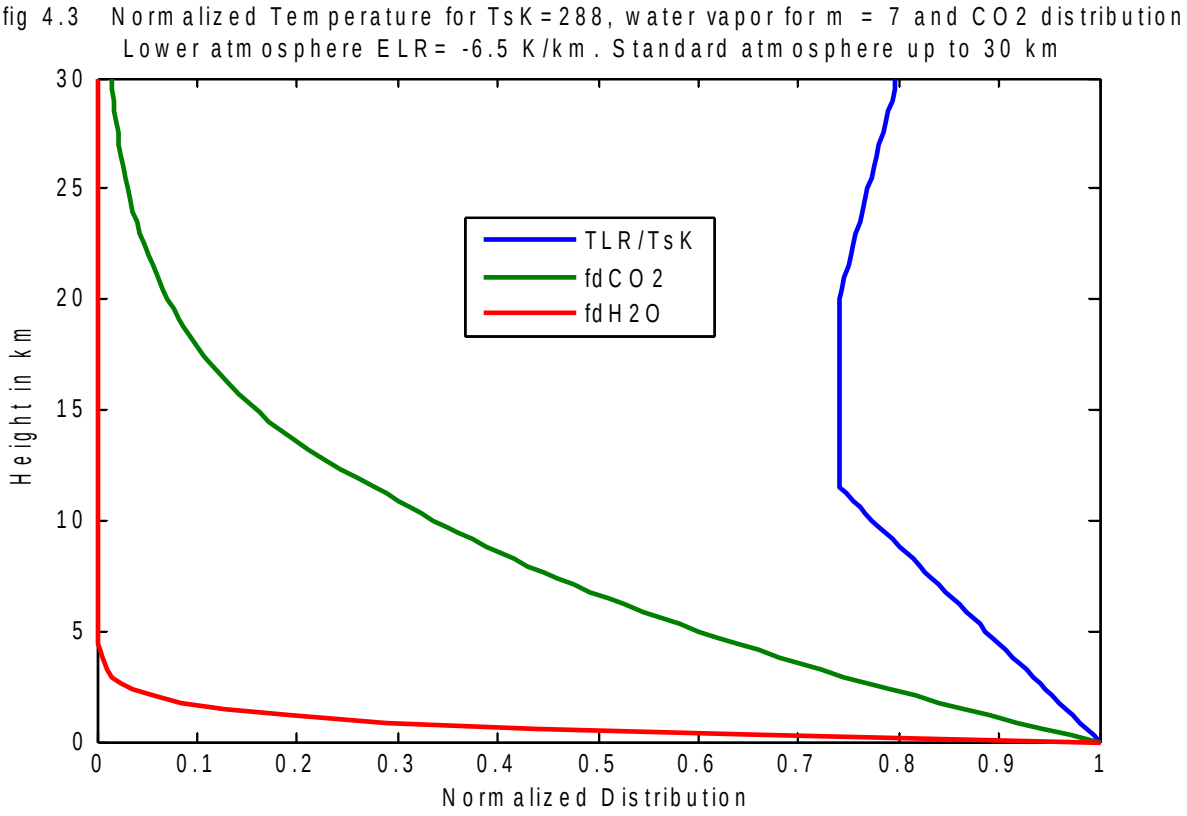

For a height up to 11.5 km the temperature is defined by the surface temperature and the environmental lapse rate , ELR = -6.5 K/km.
It is the basis of the analysis of the heat evacuation through an atmosphere with only water-vapor.
The temperature distribution is converted to the variables ϑ(i) assembled in the vector **ϑ.** With the surface temperature TsK we get TLR(i) and ϑ(i) :

TLR(i)=TsK + ELR*z(i) and ϑ(i) = σ*(TsK +ELR*z(i))^4 **(4)**

Where z(i) < 11.5 is the vertical coordinate of the grid in km.

For z(i) >11.5 km – for the CO_2 analyses -– the temperature distribution follows from figure 3, which corresponds to the standard atmosphere.
In figure 3 are also depicted the normalized distribution of H2O vapor and of CO2 : fdH2O and fdCO2, respectively.
The normalized H2O distribution is defined heuristically by an exponential drop : fdH2O(z) = exp(-m*z/height5)
The coefficient m = 7, for a reference height5 of 5 km, is obtained by comparing the results with the mainstream papers on the subject.
The CO2 distribution is taken proportional to the height dependent density in the atmosphere, assuming the volumetric concentration of CO2 is constant over the height. More details are given in **[1]**.

Fractions of H2O and CO2 in the LW terrestrial spectrum

From figure 4 we can conclude that the fraction of CO2 in the spectrum is 28 +18 =46 W/m² of the total Prevost flux = 394 W/m² for TsK= 288.72 :
fractionCO2 = 0.1168 and fractionH2O= 1-fractionCO2 = 0.8832
Figure 4 from Pangburn blog **[2]**

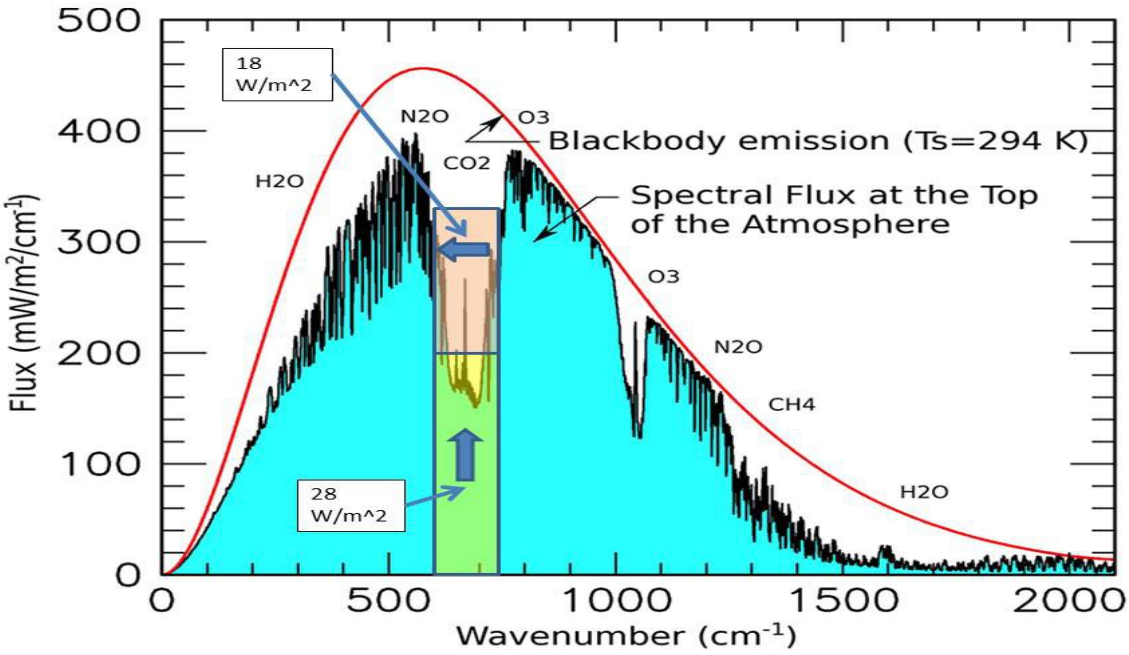

Original graph from NASA
NB Ts =294 K in figure 4 is a reference value for the red Planck curve.
Other data for a temperature of 28.7 .

Results of stack model for water-vapor.

From figure 3 we see, for the evacuation of heat through an atmosphere with only water-vapor , a model with a height of 11.5 km is sufficient.
The computer program includes a mesh generator with element sizes based on geometric series: for N=40 nodes of order of 2 meter at the surface and of 2 km at 11.5 km height.
Figure 5 gives a graphical display of the vector relation **q = K*ϑ.**
It might be useful to repeat in words what the vector relation means:
for a measured temperature distribution given in 40 nodes by a vector of parameters **ϑ** *of order 40 and by multiplication by a radiation matrix* ***K*** *of order 40x40, one obtains a vector* ***q*** *of order 40.*
What is the physical interpretation of the components of the vector **q** ?
They represent: q(1) = qsurf = LW surface flux of water-vapor
-q(N) = OLR = outgoing LW radiation of water-vapor
We see in figure 5 these two components of the vector **q** as function of ftot, being the sum of the grid coefficients f(i) : ftot =sum(**f**) – 2.

Figure 5

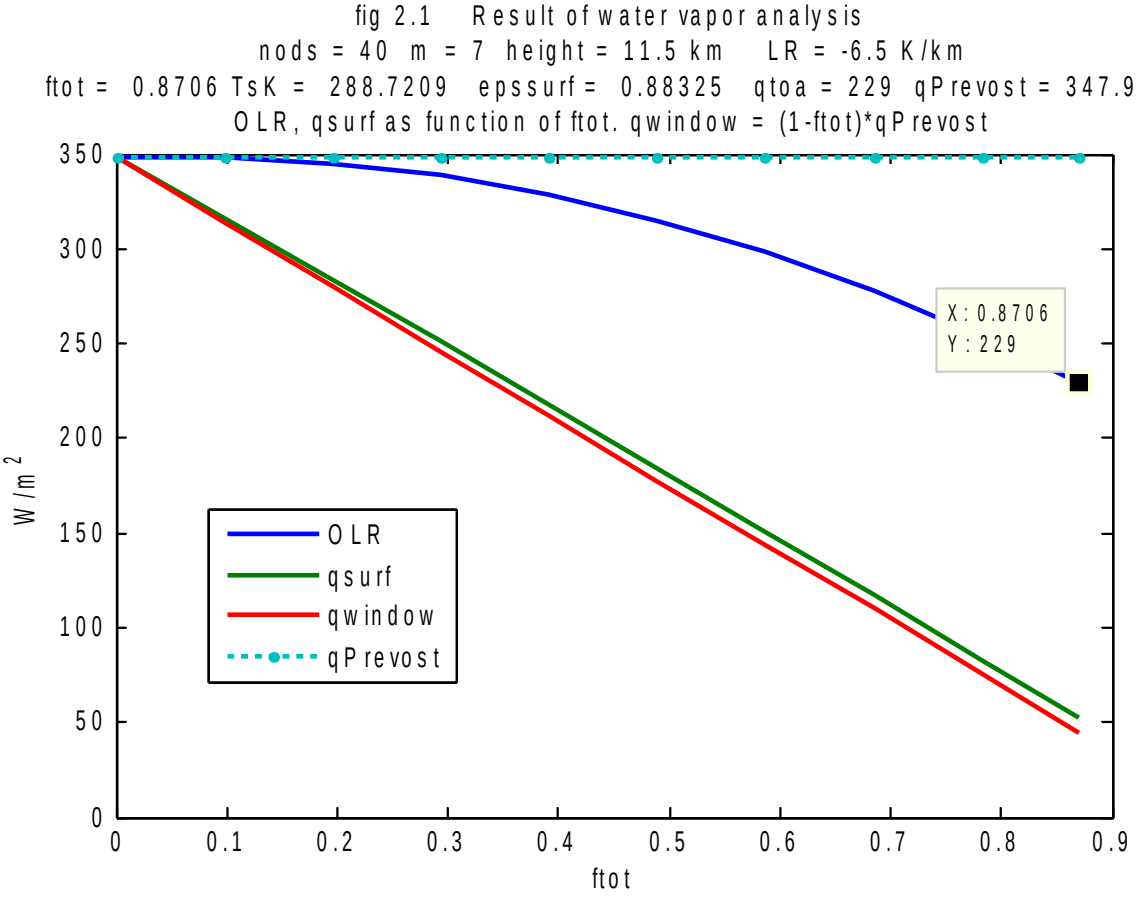

OLR_{H2O} of 229 W/m² is the average of the global outgoing LW radiation from water vapor, for which the stack model gives ftot= 0.8706 and a window of (1-ftot) = 0.1294. With OLR_{CO2} =11 W/m² from figure 8, the classical total outgoing flux at top of atmosphere, qtoa = 240 W/m².
The calculated values of the other components of **q** are given in Figure 6, not as nodal values with dimension W/m² but as distribution in W/m³.

Figure 6

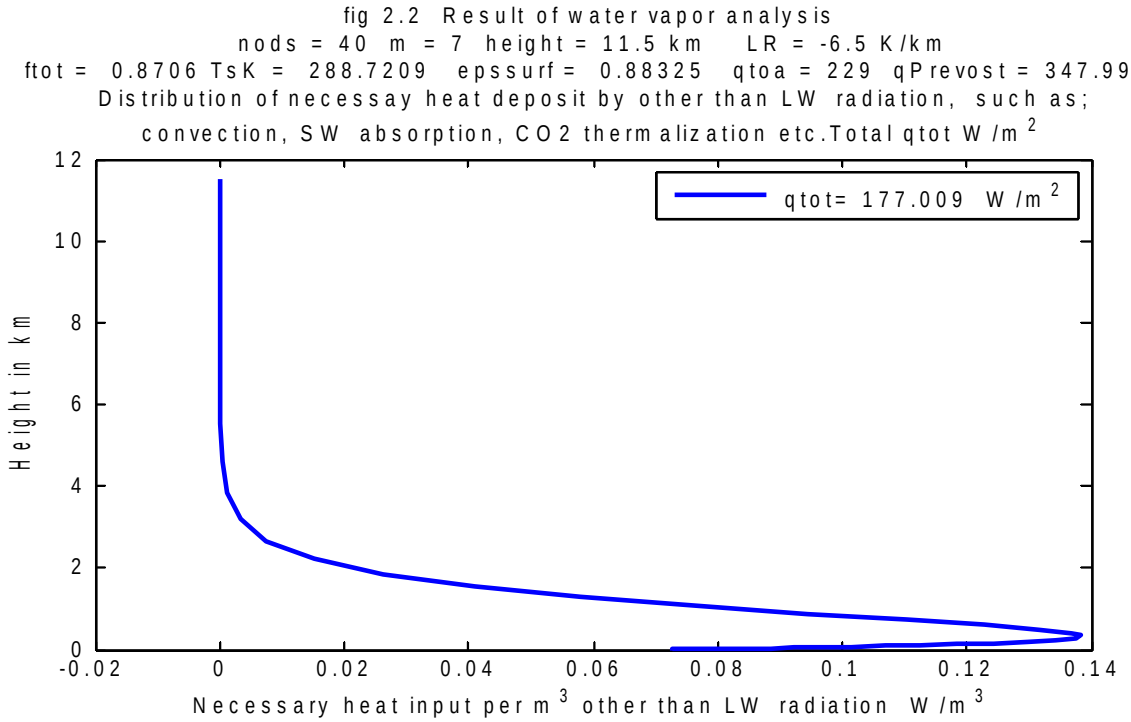

These additional sources of heat are needed, in order that the temperature distribution indeed corresponds to the measured one, shown in figure 3.
The stack model calculates, apart from LW radiation, the necessary additional heat input : 177 W/m² .
Possible other heat inputs are from:

- *absorption of incoming SW radiation by aerosols*
- *convection from the surface of sensible and latent heat,* and
- *thermalization of CO2 i.e. absorbance in the atmosphere of a part of the CO2 LW radiation from the surface but not re-emitted.*

The first two contributions are also mentioned by mainstream authors on the subject, but the third possible contribution, the thermalization of CO2, seems to be ignored. We come back on the phenomenon further on.

Dependence of OLR on surface temperature

For studies related to the dependence on the ambient temperature of the evacuation of heat from the planet by LW radiation , we need the variation of OLR with the surface temperature TsK.
We use a Taylor expansion of OLR around TsK.
For that purpose we differentiate relation **(4)** with respect to TsK:

$$TLR(i)=TsK + ELR*z(i) \quad \text{and} \quad \vartheta(i) = \sigma*TLR(i)^4 \qquad \textbf{(4)}$$

$$dTLR(i)/dTsK = 1 \quad \text{and} \quad d\vartheta(i)/dTsk = 4*\vartheta(i)/TLR(i) \qquad \textbf{(4a)}$$

The derivative of the components of the vector **ϑ (**or **theta)** with respect to TsK are assembled in a vector **dthetadTsK**.
By differentiating the stack equation **q=K*theta** we find , for constant **K:**
dqdTsK =K*dthetadTsK → component N: dOLR/dTsK = - dqdTsK(N)

The result is: dOLR/dTsK = 3.2285 = $dOLR_{H2O}/dTsK$ [W/m²/K]
We find a relation for the increase of OLR due to the surface temperature increase. We use the IPPC name for it, forcingOLR:

$$forcingOLR = (dOLR_{H2O}/dTsK)*deltaTsK \qquad \textbf{(5)}$$

In the CO2 analyses we define also a contribution from CO2:

$$forcingOLR = (dOLR_{H2O}/dTsK + dOLR_{CO2}/dTsK)*deltaTsK \qquad \textbf{(5a)}$$

Saturation of dense infra-red-active gases

In figure 7 are given the results of analyses for water-vapor concentrations with ftot>1. We see that the OLR is not decreasing any more for ftot >1. The phenomenon is called saturation and is explained by equation (2b) , repeated here:

$$viewfactor(i , j) = 1 - \sum f(k) \quad \text{with} \quad z(i)<z(k)<z(j) \qquad \textbf{(2b)}$$

For $\sum f(k) > 1$ the viewfactor(i , j) becomes negative and it is put to zero.

Figure 7

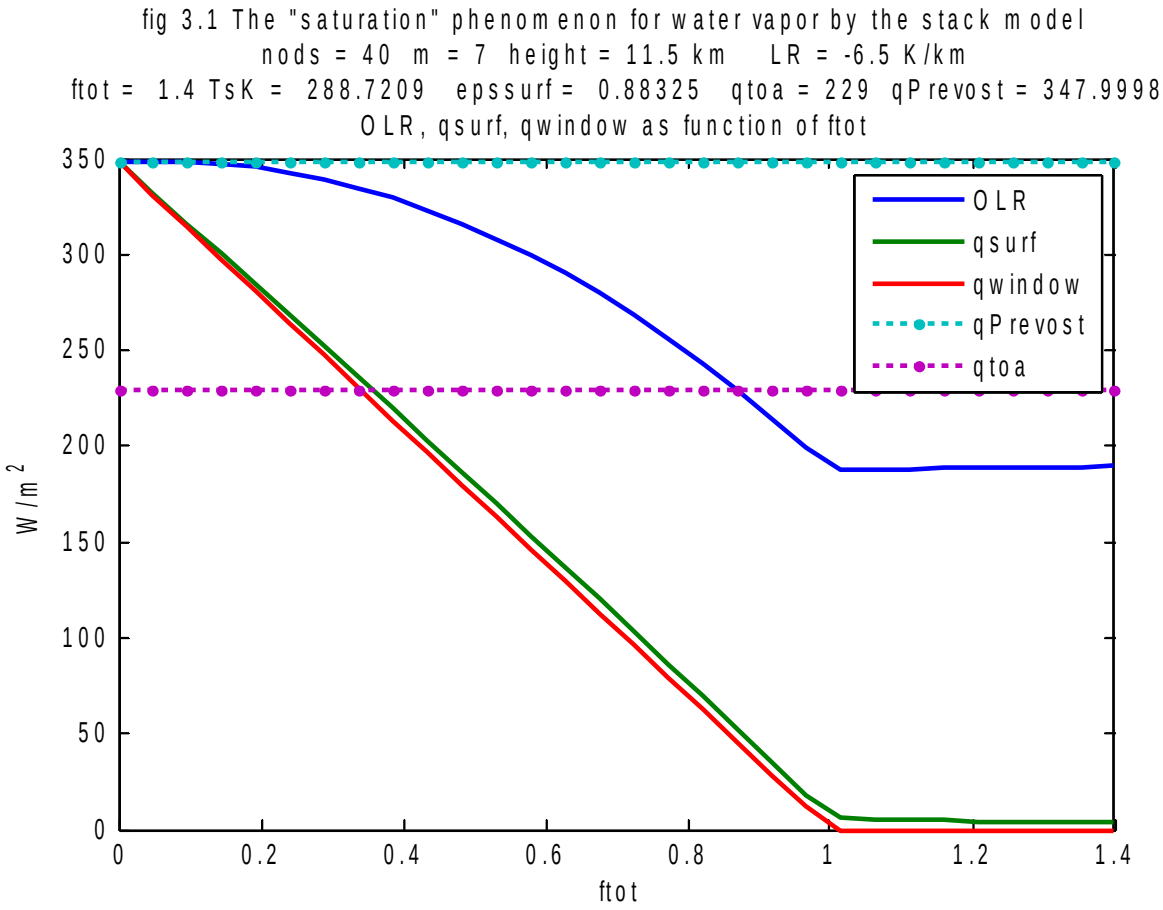

The saturation phenomenon does not appear for water-vapor with ftot <1.
It is shown here for water-vapor, for demonstration purposes only, because it is important for CO2 analyses further on, with ftotCO2 >1.
IPPC is hiding the CO2 saturation phenomenon, although it is the reason for the planet not heating up, as will be shown in the next sections.

Results of the stack model for CO2

The stack model for H2O is a one-stream, mono-chromatic model of the evacuation of heat from the planet.
It turns out to be accurate enough when compared to the results of mainstream authors on the subject, but adjusted for the nonphysical back-radiation in the two-stream models .
It can also be used for the analysis of CO2 with saturation for values of ftotCO2>1.

For the CO2 analysis we take a model with a height of 30 km with the three 3 temperature zones, according to figure 3.
We use N = 90 nodes to model the three zones : 60, 15 and 15.
The results of the vector relation **q = K*ϑ** are given in figure 8, which is equivalent to figure 5 for the water vapor analysis.
The components of **q** represent:

q(1) = qsurf = LW CO2 surface flux
-q(N) = OLR = outgoing LW CO2 radiation

Figure 8

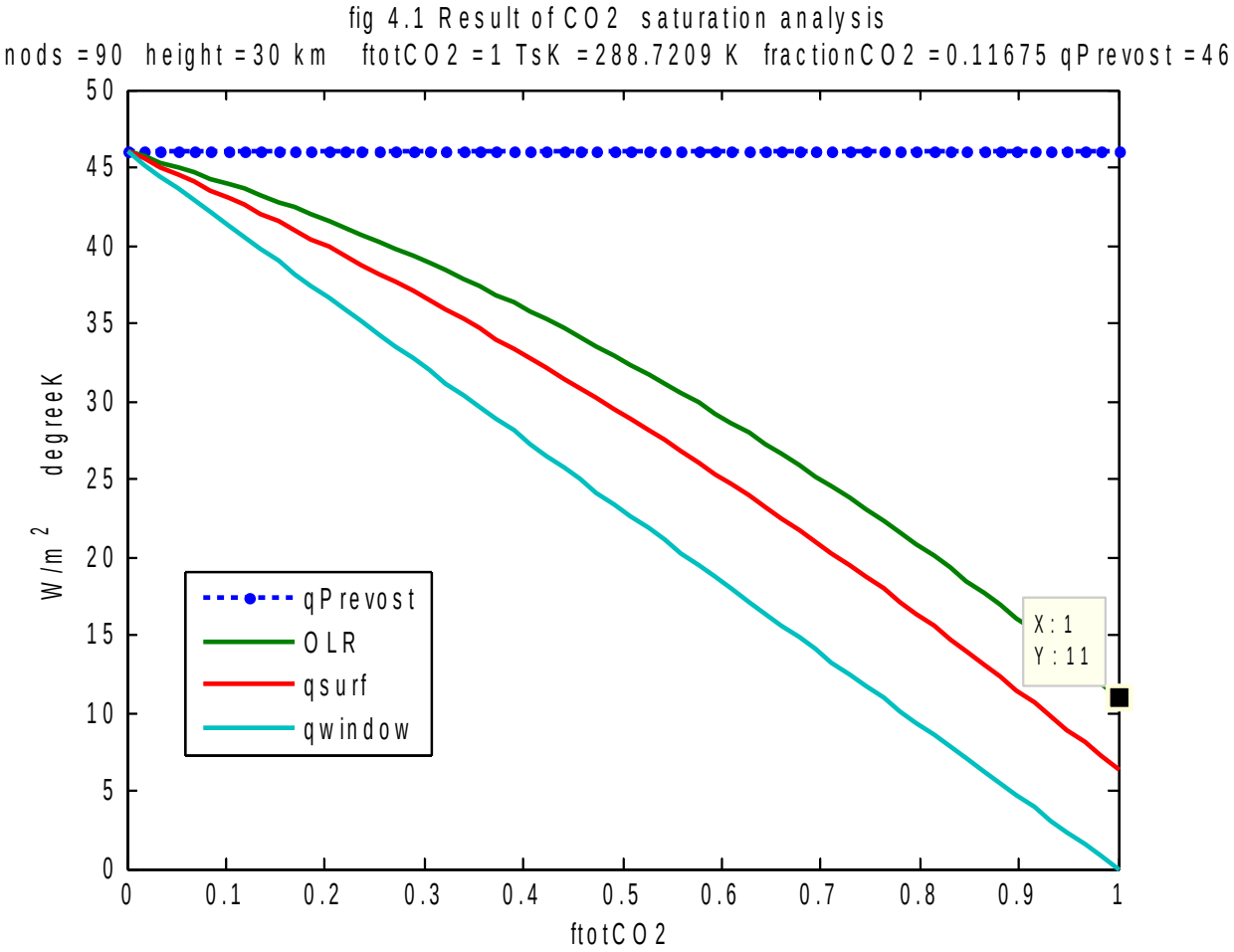

The calculated values of the other components of **q** are given in Figure 9, not as nodal values with dimension W/m² but as distribution in W/m³.
The integrated value qtot = 4.68 W/m² , can be provided by the heat from SW absorption from the Sun, and convection of sensible and latent heat from the surface.
It is equivalent to figure 6 of the water-vapor analysis.

Figure 9

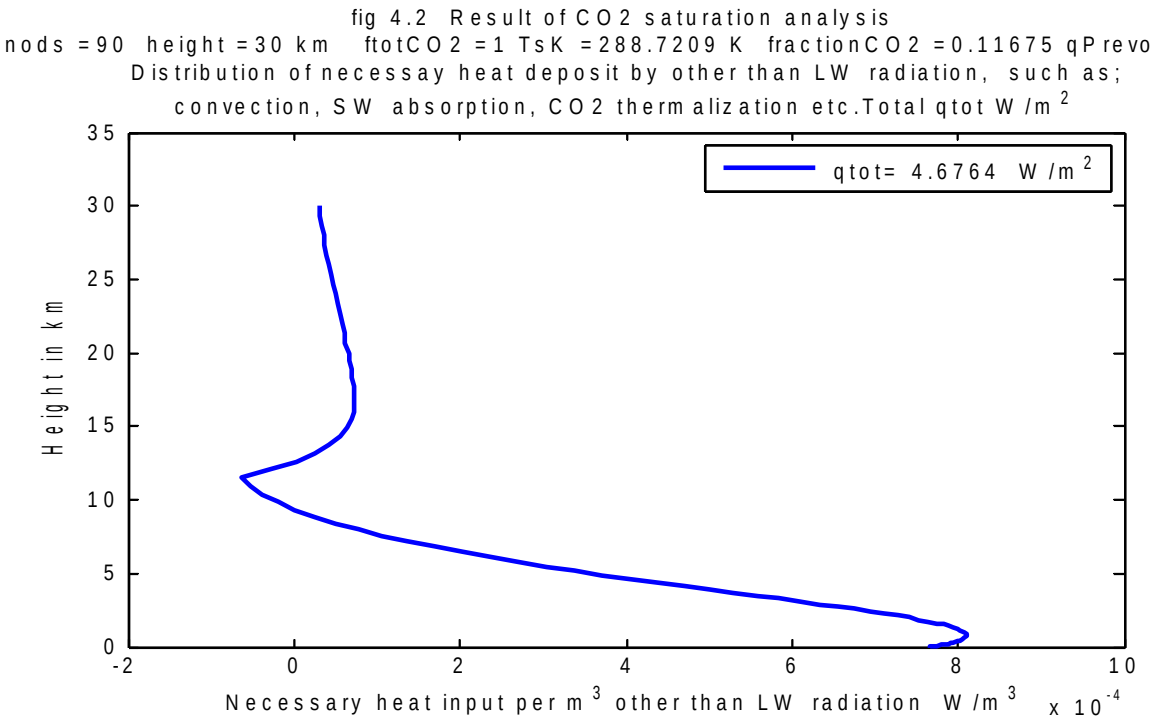

Dependence of OLR_{CO2} on surface temperature

We can define $dOLR_{CO2}/dTsK$ in the same way as for water-vapor, given in equations (4) and (4a) , also because the atmospheric temperature above 11.5 km does not depend on the surface temperature.
The CO2 influence is added to the H2O influence as already mentioned before in equation (5a) , repeated here:

$$dOLR/dTsK = dOLR_{H2O}/dTsK + dOLR_{CO2}/dTsK \qquad \textbf{(5a)}$$

$$forcingOLR = dOLR/dTsK * deltaTsK$$

The CO2 term depends on the CO2 concentration as shown in figure 10.

The relation 5a for forcingOLR with the derivative of OLR with respect to TsK - both $dOLR_{H2O}/dTsK$ and $dOLR_{CO2}/dTsK$ - governs the control of the necessary qtoa = 240 by adaptation of the surface temperature.

Figure 10

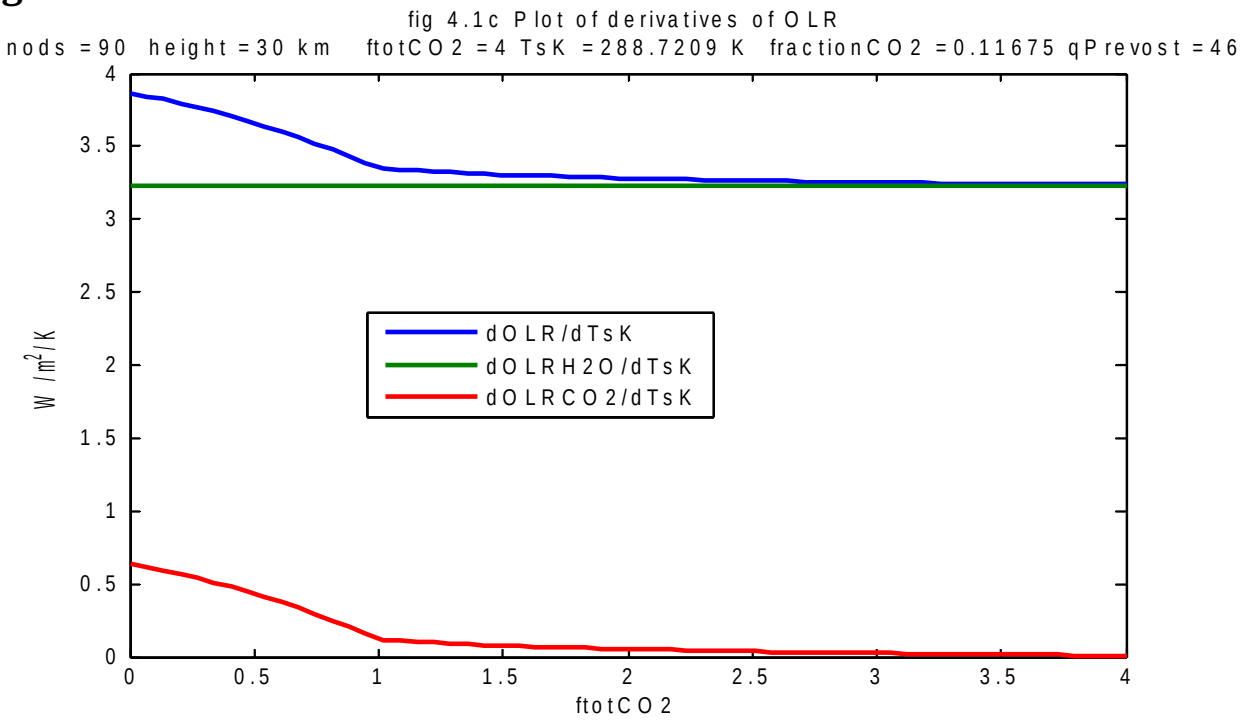

We observe that forcingOLR — i.e. the variation of OLR due to surface temperature variation — comes mainly from the contribution of water-vapor, the contribution of CO2 is reduced for fotCO2 >1 (>400ppm) due to saturation of CO2 .

Surface temperature increase due to CO2

We see in figure 8 a decreasing OLR_{CO2} flux , from qPrevost = 46 W/m² for ftotCO2 = 0 towards lower values. The decrease $deltaOLR_{CO2}$ as function of OLR_{CO2} - i.e. also a function of ftotCO2 - becomes:

$$deltaOLR_{CO2} = -(qPrevost - OLR_{CO2}) \quad \textbf{(6)}$$

In order to keep the total OLR constant, the necessary increase of OLR due to the increase of the surface temperature TsK, called forcingOLR, is the opposite: forcingOLR = $- deltaOLR_{CO2} = (qPrevost - OLR_{CO2})$
With the corresponding temperature increase from equation (5a) :

$$deltaTsK = forcingOLR / (dOLR/dTsK) \quad \textbf{(5a)}$$

Figure 11 shows the stack results of equations **(6)** and **(5a)**.

Figure 11

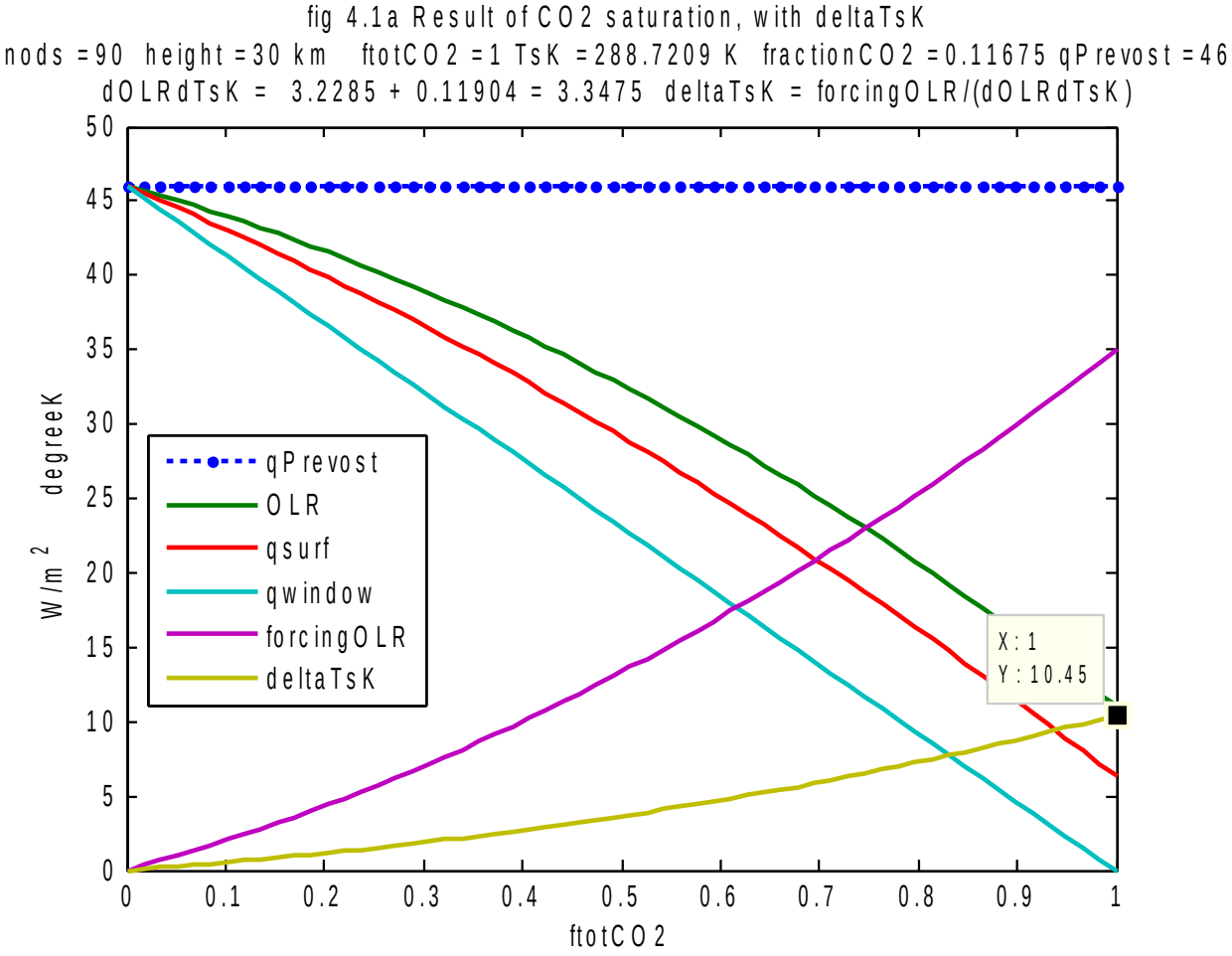

We see the curve forcingOLR for ftotCO2 = 0 to 1, giving values from zero to 35 W/m², and the corresponding curve for deltaTsK from zero to 10.45 K.
The author lives in France and he remembers himself the 24/7 screen-wide slogan on French national TV, during 2015 IPCC COP21 in Paris:

$$\Delta F = \alpha \ ln(C/C0)$$

A logarithmic increase of the forcing, referring to forcingOLR in figure 11, according to IPPC. National TV was used to indoctrinate the public.
Indeed, beyond ftotCO2 = 1 which corresponds to the 400 ppm of the year 1990 AD *already 25 years before* the fake slogan of COP21 in Paris, there is saturation, as shown in figure 12.

figure 12

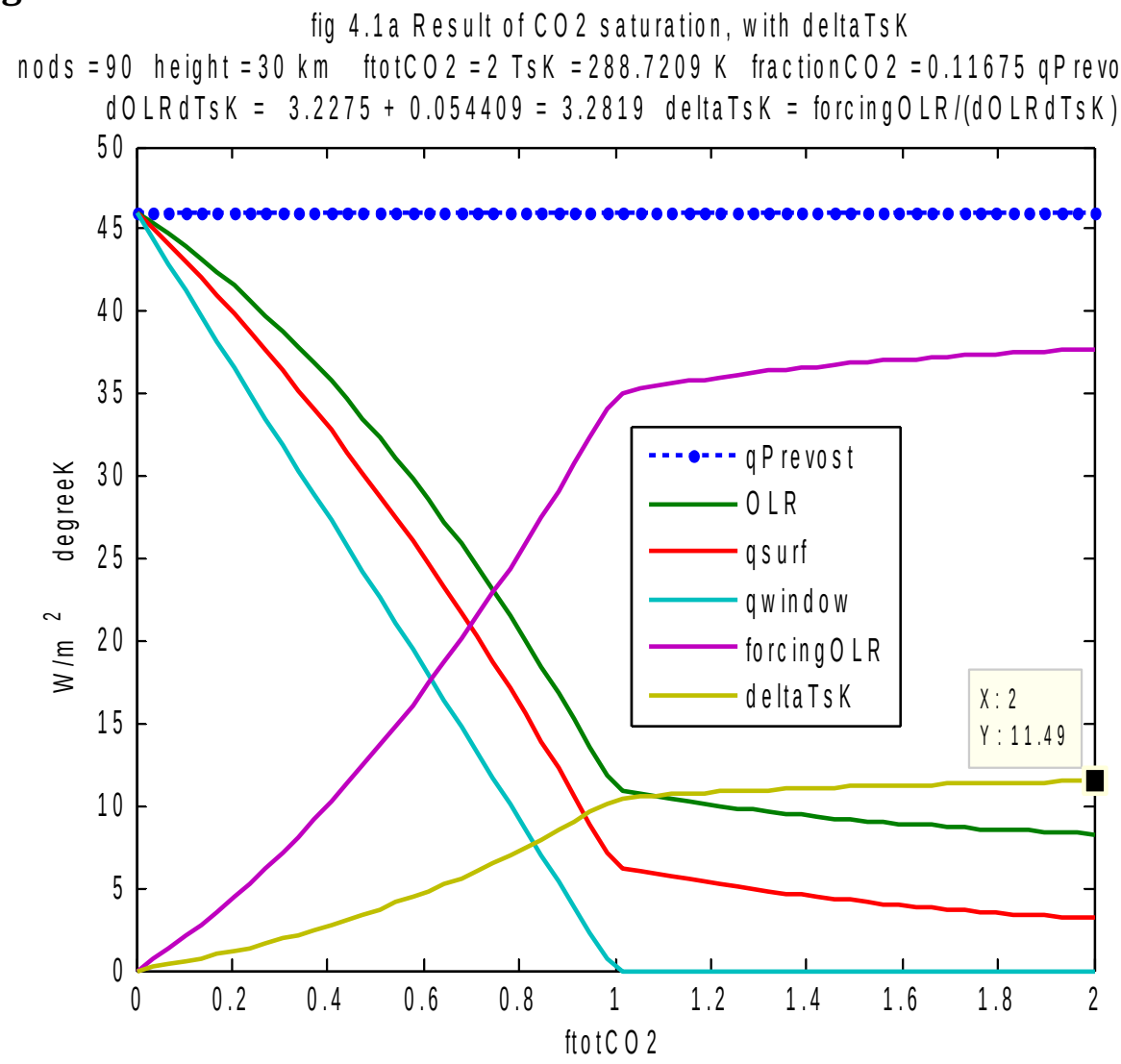

The increase of deltaTsK from ftotCO2 = 1 to 2 : 11.49 – 10.45 = 1.04 K.

The present CO2 concentration of 420 ppm corresponds to ftotCO2 = 1.05. With the present rate of CO2 increase, ≈ 0.6 ppm/yr , we will have ftotCO2 = 2 or 800 ppm in the year 2657 AD.

Comparison with the results of William Happer

Happer **[4]** in figure 13 finds also that the *variation* of temperature increase due to CO2 remains low in the saturation region for fotCO2>1. Both Happer and stack results are for surface temperature TsK = 288.72 .

Figure 13 From Happer **[4]**

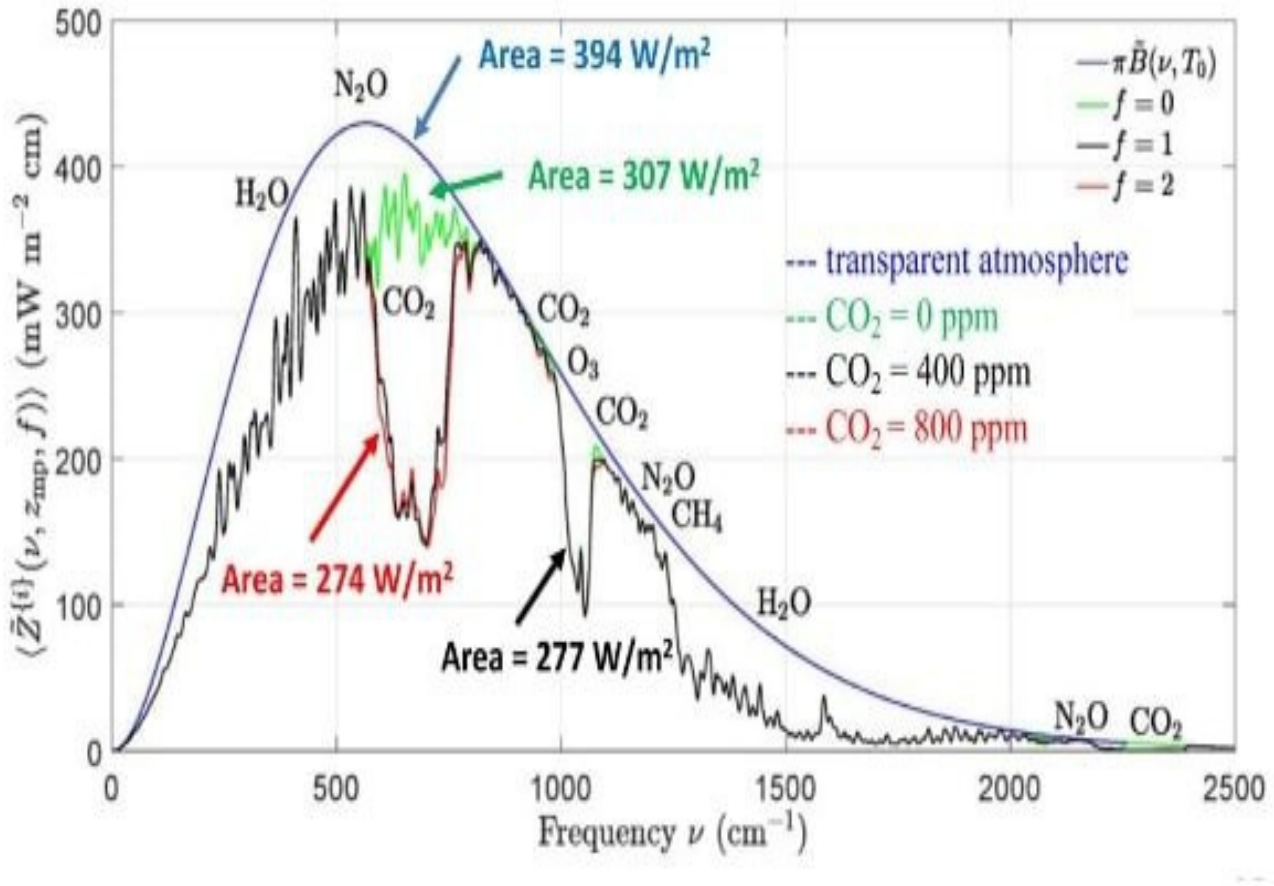

In Table 1 the results of the stack model from figure 12 are compared with the results from Happer from figure 13 .
The Happer nomenclature is different from the stack nomenclature:
f in Happer corresponds to ftotCO2 in the stack model,
deltaArea in Happer corresponds to forcingOLR in the stack model.

Table 1 Comparison between stack results and Happer results.

		stack results		Happer results	
ftotCO2 or f	ppm	forcingOLR	deltaTsK	deltaArea	deltaTsK(H)
0	0	0	0	0	0
1	400	35	10.45	30	9.12
2	800	37.7	11.49	33	10.03
difference (2) -(1)		2.7	1.04	3	0.912

The blue line represents differences between 800 ppm and 400 ppm
NB deltaTsK(H) from Happer is obtained using the stack relation **(5a)** :
deltaTsK(H) = deltaArea/3.289

Stack saturation results for higher CO2 concentrations

Figure 14 gives results of the stack model for values of ftotCO2 up to 8. *The value ftotCO2 = 8 is only given to show that after ftotCO2 =4 the numbers do not change anymore*.

Figure 14

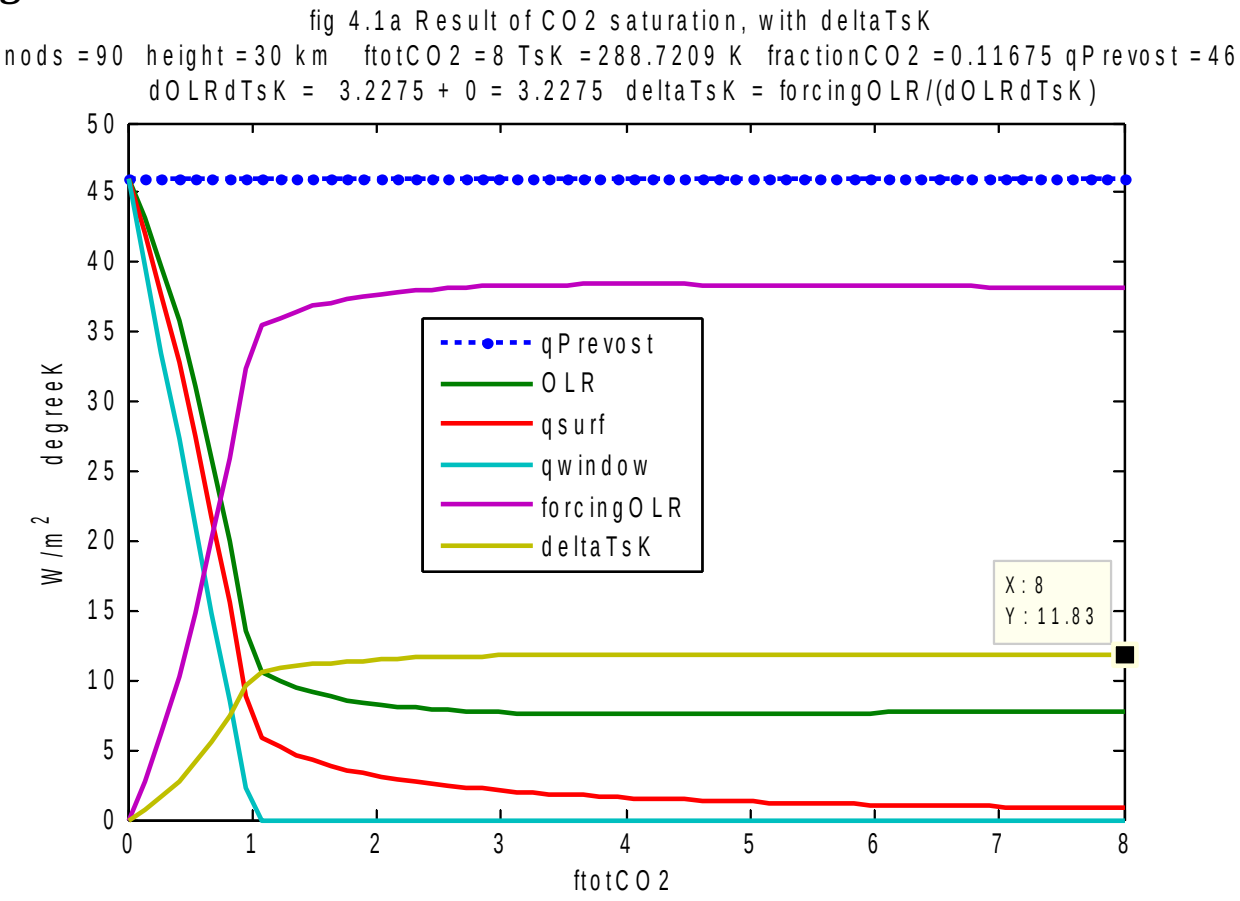

In Table 2, are given the temperature increases deltaTsK, from figures 11, 12 and 14 , including the **relative** increases from the value 10.45 K for a CO2 concentration of 400 ppm in the year 1990 AD.

Table 2 Temperature increase due to fotCO2 = 0 to 8.

ftotCO2	ppm	deltaTsK	deltaTsK– 10.45	year AD
0	0	0		
1	400	10.45	0	1990
2	800	11.49	1.04	2657
4	1600	11.87	1.4	?
8	3200	11.83	1.38	?

Effect of the thermalization of CO2

The classical Stefan-Boltzmann relation **(1)** assumes that the information exchange concerning the temperatures between surfaces and thereby exchange of energy is immediate. But the relaxation time – i.e. the time between absorption and emission - is not exactly zero. In particular for the infra-red-active molecule CO_2 with three "heavy" atoms - one C-atom and two O-atoms - the relaxation time is large as compared to the time between collisions of molecules. Before a CO_2 molecule has completely built up the necessary surplus energy level for emission, it could lose the surplus energy by collision with other molecules : 80% nitrogen N_2, 19% oxygen O_2, and other trace gases such as water-vapor. The CO_2 molecule is said to be thermalized, the surplus energy goes to the bulk of the molecules of the atmosphere and it uses the H2O radiation path to outer space according to Figure 6.
See figure 4 and Pangburn blog **[2]** for further details
The phenomenon has been confirmed to the author by le Pair [3].
It is obvious that the one-stream stack model, does not leave space in the balance for an eventual thermalization deposit into the bulk of the atmosphere.
In the Pangburn figure 4 we see OLR CO2 = 28 W/m² and a heat deposit due to thermalization into the bulk of the atmosphere of 18 W/m² .
Following the CO@ analyses , we see a necessary forcingOLR of an amount of 46 – 28 = 18 W/m ².
According to relation **(5):** deltaTsk = 18 / 3.289 = 5.47 K.
Pangburn has given one single result for 400 ppm.
When we introduce that value in Table 2 and we assume - in blue - it will not change for higher ppm's, we get Table 3.

Table 3 Temperature increases from fotCO2 = 0 to 2 .

		saturation		*thermalization*	
ftotCO2	ppm	deltaTsK	deltaTsK – 10.45	deltaTsK	deltaTsK – 5.47
0	0	0		0	
1	400	10.45	0	5.47	0
2	800	11.49	1.04	5.47	0

When the OLR due to thermalization for ftotCO2 >1 will not change, there is zero additional temperature increase compared to the results for 400 ppm CO2.

Conclusions

The one-stream, chicken-wire stack model for infra-red-active trace gases, already validated for the analysis of LW radiation through an atmosphere with water-vapor, has now also been applied to the analysis of CO2 gas. The stack model deals with the issue of saturation of CO2 in a transparent way, giving a limited increase of the surface temperature for CO2 concentrations beyond ftotCO2 = 1 or 400 ppm.
These results of the one-stream stack model in figure 12 are similar to the results reported by Happer in figure 13.

Both results are much smaller than the fake alarmist IPPC numbers, with the fake slogans during COP21 in 2115 in Paris and also more recently, to indoctrinate the innocent public, including children.

Thermalization of CO2 as reported by Pangburn and confirmed by le Pair give even lower temperature increases as compared to the saturation analyses. Pangburn has given experimental results for 400 ppm, further studies for higher CO2 concentrations will certainly confirm that due to thermalization of CO2 the planet is not heating up due to CO2.

Acknowledgment

The author wants to thank Claes Johnson [6] who inspired him to write this paper based on the one-stream LW radiation to outer space, avoiding the nonphysical back-radiation.
The author interpreted the one-stream proposals from Johnson by using the Stefan-Boltzmann relation all ways for a pair of surfaces, enabling the concept of standing waves between resonating infra-red-active molecules with the same eigenfrequency.

Thanks to Dan Pangburn and to William Happer for their authorization to include figures from [2] respectively [4] in this paper.

The author expresses his gratitude to John O'Sullivan for hosting this paper on Principia Scientific.

References

[1] https://principia-scientific.com/publications/Reynen-Finite.pdf
[2] Pangburn blog https://www.researchgate.net/publication/316885439_Climate_Change_Drivers
[3]Private communication 10/11/2021 from C. le Pair, The Netherlands.
[4]Happer, https://www.youtube.com/watch?v=PblYr-KjOVY
[5] https://principia-scientific.com/wp-content/uploads/2021/12/SaturationFinal-rev.pdf
[6]https://computationalblackbody.wordpress.com/